Influence of supercritical CO_2 flowrate in one-pot supercritical fluid extraction of *Carica papaya* linn. leaves: A broken-intact-cell approach

Yee Ho Chai[1], *Suzana* Yusup[1,2], *Qiu Huan* Seer[3], *Muhammad Syafiq Hazwan* Ruslan[2] and *Bridgid Lai Fui* Chin[3]

[1]Biomass Processing Laboratory, HICoE-Centre for Biofuel and Biochemical Research, Institute for Self-Sustainable Building, Department of Chemical Engineering, Universiti Teknologi PETRONAS, 32610, Seri Iskandar, Perak, Malaysia
[2]Department of Chemical Engineering, Universiti Teknologi PETRONAS, 32610, Seri Iskandar, Perak, Malaysia
[3]Department of Chemical Engineering, Faculty of Engineering and Science, Curtin University Malaysia, CDT 250, 98009, Miri, Sarawak, Malaysia

Abstract. The presence of rich phytochemicals in *Carica papaya* linn. leaves are potentially beneficial in pharmaceutical, nutraceutical and food industries. This work aims to investigate the roles of solvent flowrate for the predictive behaviour of supercritical fluid extraction of essential oil-rich extracts by broken-intact-cell modelling approach. Through kinetic model fitting of experimental data, the adjustable parameters namely G, φ_k, Z and Y were determined through error minimization procedure. From the cumulative extraction curve at solvent rate from 4 – 8 mL/min, the values of mass transfer coefficients were in the range of 4.40 x 10^{-5} m^2/s – 19.92 x 10^{-5} m^2/s with an overall relative 8.67% AARD. The grinding index and end of fast extraction time period was within the range of 0.144 – 0.258 and 30.38 – 91.17 min respectively. The role of solvent flowrate played an influential role in the extraction of papaya leaves extract.

1 Introduction

In the effort to replace conventional extraction methods such as steam distillation and solvent-based techniques, the drawbacks of conventional extraction techniques, such as thermal degradation, high consumption of organic solvents and non-specific compound extractions, have favoured supercritical fluid extraction (SFE) technology for the extraction of value-added bio-compounds from biomass resources. The use of carbon dioxide as an extractive solvent in SFE technology are non-toxic, non-flammable, low critical points, low costs, recyclable and reduced solvent consumption [1] are attractive properties compared to conventional extraction techniques. The absence of oxygen in the recovery process also avoids the degradation of antioxidants presence in various bioactive compounds [2]. This has paved ways for major applications of SFE technology especially in valorisation of biomass resources into value-added bioproducts.

Carica papaya linn. (papaya) leaves contain various bioactive compounds such as alkaloids, flavonoids, terpenoids, and saponins that possess medicinal properties. Papaya leaf extracts contain therapeutic effects such as decreased cardiovascular disease risks, healing of wounds, curing fever and diabetes mellitus [3,4]. Besides that, papaya leave barks contain acetogenins that possess anti-tumour properties in curing cancer [5]. Furthermore, bioactive compounds presence were discovered to be effective in repelling mosquitoes transmitting dengue fever, malaria and filariasis [6]. However, literature review on SFE of papaya leaves are seldomly reported and the lack of literature information in modelling of SFE from papaya leaves prompted an initial study on the effects of operating physical parameters on the recovery of essential oil in this study. Broken-intact-cell (BIC) model was selected as the model is able to provide an accurate description for pretreated milled plant matrices that takes into account the structure of biological material and the extraction limitations imposed in a SFE process.

The aim of this paper was to evaluate the roles of physical operating parameters, namely temperature, pressure, solvent flowrate and particle size, on the SFE of papaya leaves. The mathematical modelling conducted is essential in the understanding of physical properties of papaya leaves and its limitation imposed in this study.

2 Materials and methods

2.1. Sample preparation

Papaya leaves were collected from local homegrown papaya plants and were washed with water to eliminate any solid impurities presence on the leaves' surface. The washed leaves were subjected to natural drying under direct sunlight for 3 hours before oven dried at 50°C for 24 hours to remove remaining moisture trapped. The leaves were ball-milled into powder form within micrometre range through ball-milling procedure

* Corresponding author: drsuzana_yusuf@utp.edu.my

(Planetary Micro Mill PULVERISETTE 7 *premium line*). The powdered leave samples were stored in the refrigerator at 5°C until further use.

2.2. Supercritical fluid extraction (SFE) process

The experimental procedure carried out and consumables used in this study followed the procedure outlined by Chai et al. [7]. For this study, the BIC model was used to model the mass transfer phenomenon of supercritical CO_2 (SCO_2) into papaya leaves on how the variation of each parameter affects the extraction process. The scope of boundary for each parameter was outlined in Table 1 below. The results obtained were compared against the optimized results obtained by Chai et al. [7].

Table 1. Boundary for operating ranges of SFE of papaya leaves.

Parameter	Scope of boundary
Temperature	57.47°C
Pressure	15 – 35 MPa
Solvent flowrate	4 – 8 mL/min

2.3. Broken-intact-cell (BIC) model

In this study, the mathematical model proposed by Sovová [8] was used to model the mass transfer approaches of SCO_2 into powdered papaya leaves with presence of co-ethanol solvent. The concept of BIC model demonstrated the presence of two regions in any plant matrices, namely broken cells as a result of grinding, milling or crushing process during pre-treatment step; and solutes present in non-damaged intact cells. The extraction periods by SFE can be distinguished into three different periods by BIC model – constant extraction rate (CER), falling extraction rate (FER) and diffusion-controlled (DC) period respectively. In BIC model, the following assumptions hold true to describe the extraction procedure from plant matrices via SFE process:
- the extraction system is isobaric and isothermal,
- the particle sizes in the system and solutes presence in each plant matrices are uniformly distributed,
- the particles contain broken cells located nearer to the surface and intact cells located towards the core,
- the extraction bed characteristics due to reduction in solid mass, including void fraction and specific surface area, remained unchanged throughout the extraction,
- the physical properties of fluid remained unchanged during extraction and,
- no solute accumulation in the extractive solvent within the system.

The mass balance equations of Sovová's BIC model was provided by the following equation:

$$\frac{E}{Nx_0} = \begin{cases} \varphi[1-e^{-\mathrm{Z}}] \text{ for } \varphi < \dfrac{\mathrm{G}}{\mathrm{Z}} \\ \varphi - \dfrac{\mathrm{G}}{\mathrm{Z}} e^{\mathrm{Z}(h_k-1)} \text{ for } \dfrac{\mathrm{G}}{\mathrm{Z}} \le \varphi \le \varphi_k \\ 1 - \dfrac{1}{\mathrm{Y}} \ln\left\{1 + (e^{\mathrm{Y}}-1)\, e^{\mathrm{Y}\left(\frac{\mathrm{G}}{\mathrm{Z}}-\varphi\right)}.(1-\mathrm{G})\right\} \\ \text{for } \varphi \ge \varphi_k \end{cases} \quad (1)$$

The recovery of oil (g oil extracted/g oil presence in bed) is defined by E (extract yield), N (mass of oil-free solid phase) and x_0 (fraction of mass of easily extracted solute/mass of insoluble solid). In practical, $x_0 = x_0 + x_k$ where x_p and x_k is the fraction of the easily extracted solute and fraction of inaccessible solute respectively. The grinding efficiency, G, is a constant dependent on solute solubility, relative solvent consumption and fraction of solute concentration in bed that can be easily estimated by simplified model proposed by [9].

The recovery of extract solute is a function of φ (dimensionless time) which can be defined as:

$$\varphi = \frac{tQy_r}{Nx_0} \quad (2)$$

where t is extraction time, Q is solvent flow rate and y_r is the solubility curve located in the first extraction period (G/Z). For the second extraction period, two regions co-exist within the extraction system between dimensionless time G/Z to φ_k, where φ_k represents the dimensionless time when all oil in the solid bed is completely extracted and can be given as:

$$\varphi_k = \frac{\mathrm{G}}{\mathrm{Z}} + \frac{1}{\mathrm{Y}} \ln\left(1 - \mathrm{G}[1-e^{\mathrm{Y}}]\right) \quad (3)$$

The dimensionless axial coordinate, h_k represents the boundary between both regions where easily and difficult solutes are extracted. Beyond dimensionless time φ_k, the difficult solutes are being extracted. The expression of h_k can be represented as follows:

$$h_k = \frac{1}{\mathrm{Y}} \ln\left(1 + \frac{\left\{e^{\mathrm{Y}\left(\varphi - \frac{\mathrm{G}}{\mathrm{Z}}\right)} - 1\right\}}{\mathrm{G}}\right) \text{ for } \frac{\mathrm{G}}{\mathrm{Z}} \le \varphi \le \varphi_k \quad (4)$$

The dimensionless variables Z and Y are dimensionless parameters which are important to determine mass transfer coefficients of fluid and solid phases. Both variables are often proportionate to the mass transfer coefficients where:

$$Z = \frac{Nk_f a \rho_f}{Q(1-\varepsilon)y_r} \quad (5)$$

$$Y = \frac{Nk_s a x_0}{Q(1-\varepsilon)y_r} \quad (6)$$

Therefore, by pre-determining the grinding efficiency (G) in Eq. 1, the adjustable parameters in the model can be reduced into three parameters (Z, Y and h_k) that were optimized by minimization of errors between experimental and modelled data sets. The average absolute relative deviation (AARD) values are reduced to minimum for the best extraction performance behaviour, where AARD can be outlined as:

$$\text{AARD (\%)} = \frac{1}{n}\sum_{i=1}^{n}\left|\frac{y_{exp} - y_{model}}{y_{exp}}\right| \text{ x } 100 \qquad (7)$$

where n is the number of experimental data sets, y_{exp} and y_{model} is the experimental data and calculated data obtained from the model respectively. The determination of mass transfer coefficients in solvent phase and solid phase, $k_f a$ and $k_s a$ were determined from data fitting using optimised Z and Y parameters in Eq. 5 and Eq. 6.

For this study, the bulk density (ρ_{bulk}) and solid density (ρ_{solid}) of the leaves were 684 kg/m^3 and 1010.31 kg/m^3 respectively which were determined through density pycnometry analysis. The value of bed void fraction was 0.323 and can be calculated through the following:

$$\varepsilon = 1 - \frac{\rho_{bulk}}{\rho_{solid}} \qquad (8)$$

3 Results and discussion

3.1. Solubility of extracts

The effect of extractive solvent flowrate from 4 to 8 mL/min for the extraction of papaya leaves extract was investigated at optimized parameters temperature of 57.47°C, dynamic extraction time of 60 minutes and co-solvent ratio of 4.98 vol%. The extraction rate was observed to be generally proportionate to the solvent flowrate as observed in Fig. 1. The maximum extract yield obtained in this study was 0.1188 g at 8 mL/min and 30 MPa. Table 2 summarized the variations of mass transfer coefficients with respect to pressure and solvent flowrate modelled by BIC approach.

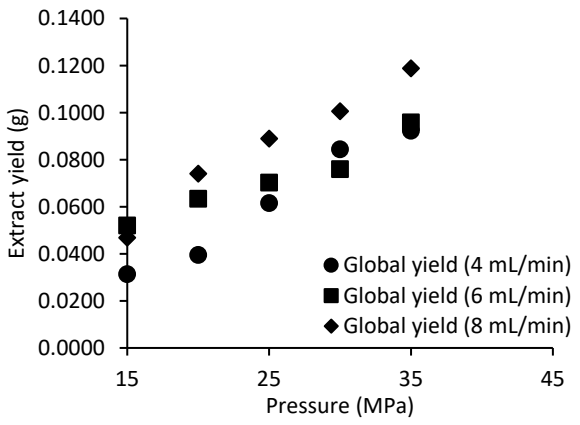

Fig. 1. Extract yield as a function of solvent flowrate and pressure.

From Table 2, mass transfer coefficient of fluid phase increases with solvent flowrate. By increasing the solvent flowrate, it reduces mass transfer resistances for the diffusivity of oil from the leaves into the solvent [10]. The decrease of mass transfer resistance was attributed to the increased in contact between solvent flowrate and local particles [11] and the decrease of surrounding film thickness [12]. Interestingly, the mass transfer in fluid phase remained constant regardless of the pressure imposed to the system as solvent flowrate as the governing parameter remains constant at various pressure. The mass transfer coefficients of solid phase were observed to increase with respect to solvent flowrate and pressure. Elevation of pressure improved the solvation power of SCO_2 within the extractive system to produce driving force into the papaya leaves matrices [13]. Furthermore, the influence of solvent flowrate had also substantially improved the mass transfer phenomenon within the papaya leaves matrices to promote intraparticle diffusion and effectively transported solutes outwards from the intact cells.

Table 2. Mass transfer coefficients and solubility of extracts with respect to flowrate and pressure

Solvent flowrate, Q (mL/min)	Pressure, P (MPa)	External mass transfer coefficient, $k_f a$ (m^2/s)	Internal mass transfer coefficient, $k_s a$ (m^2/s)	AARD (%)
4	15	0.016809	0.00009	4.90
	20	0.016809	0.00011	
	25	0.016809	0.00012	
	30	0.016809	0.00012	
	35	0.016809	0.00013	
6	15	0.031765	0.00031	4.40
	20	0.031765	0.00037	
	25	0.031765	0.00040	
	30	0.031765	0.00042	
	35	0.031765	0.00043	
8	15	0.042354	0.00060	4.31
	20	0.042354	0.00070	
	25	0.042354	0.00076	
	30	0.042354	0.00080	
	35	0.042354	0.00083	
Overall AARD (%)				4.54

3.2. Kinetic modelling

The study was extended to investigate the effects of solvent flowrate on cumulative extraction yield in the range of 4 to 8 mL/min. The optimized parameters carried out were temperature of 57.47°C, pressure of 26.62 MPa, co-solvent ratio of 4.98 vol% and maximum extraction time of 180 minutes. Fig. 2 showed the cumulative extraction yield curve plotted as a function of time by

variating the solvent flowrate. The solvent mass flowrate for 4, 6 and 8 mL/min respectively were 0.054, 0.081 and 0.108 g/s respectively. The density of SCO_2 for this study was considered constant at 808.11 kg/m^3 regardless of flowrate varied. Table 3 highlights the important extraction parameters required for the BIC model calculation in this study.

Table 3. Extraction parameters required for model calculation.

Parameters	**Units**	
Density SCO_2	808.11	kg/m^3
Solvent dynamic viscosity	0.00007	Pa.s
Volumetric flow	1.333 x 10^{-7}	m^3/s
Solvent flow rate (Q)	0.1077	g/s
Solubility (y_r)	5.8 x 10^{-4}	g oil/g CO_2
Mass loading	1.5 x 10^{-3}	kg
Mean particle dia.	3.2 x 10^{-4}	m
Specific surface area	18,986.74	1/m
Bulk density	684.00	kg/m^3
Solid density	1010.31	kg/m^3
Bed void fraction (ε)	0.32	
Insoluble solid (N_m)	1.24	g
Mass Loading (N)	1.50	g
X_0	0.21	
X_p	0.15	
x_k	0.06	

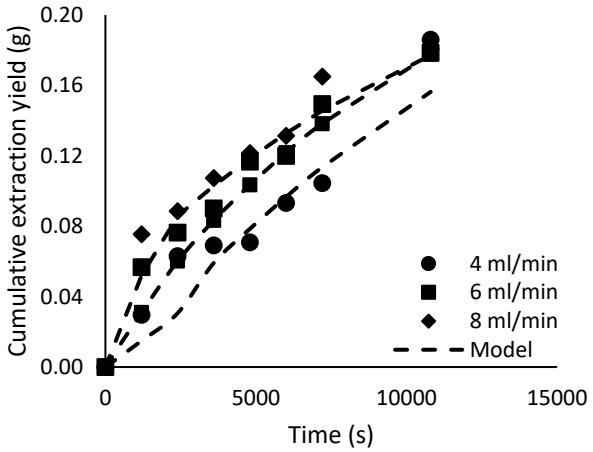

Fig. 2. Cumulative extraction curve as a function of time.

From Fig. 2, the overall extraction curves are proportionate to solvent flowrate where higher extraction yield are obtained at higher solvent flowrate. The cumulative extraction curves were observed to approach asymptotic value at the end of each experiment which indicated the exhaustion of easily accessible solutes present in the diffusion-controlled dominated region. However, it should be noted that introduction of excessive high solvent flowrate into the system may not saturate the solvent exiting the extractor as excess solvent will bypass the plant matrices as a result of intraparticle diffusion resistance limitation [14]. Fig. 3 illustrated the extraction rates of all experiments were independent of solvent flowrate at the initial stage due to the high concentration of solutes present especially in the broken cell region. The governing extraction mechanism in the initial stage (constant extraction rate) was mainly convection between extraction solvent and easily accessible solutes [15].

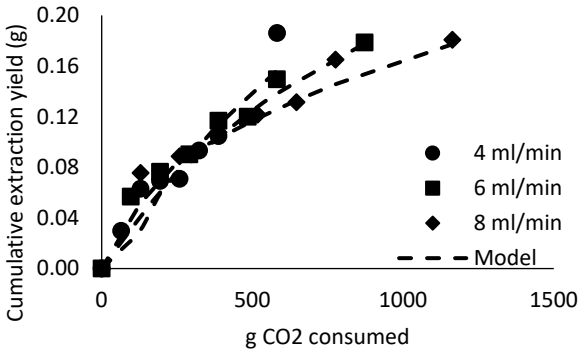

Fig. 3. Cumulative extraction curve as a function of SCO_2 consumed.

Interestingly, the mass transfer coefficients, k_fa and k_sa, do not synonymously increase with solvent flowrate as reported by other researchers [16,17]. Fluid phase mass transfer coefficients (k_fa) were observed to increase with solvent flowrate as expected due to the increase number of CO_2 molecules entering the extractor. However, solid phase mass transfer coefficients (k_sa) decreased at higher solvent flowrate. A plausible explanation to this observation can be attributed to the irregular particle sizes used as fixated particle sizes were unaccounted for in this study. Furthermore, the inclusion of co-solvent ethanol may play an influential role in k_sa determination. The volume of co-solvent increased with SCO_2 flowrate introduced into the system. As a result of higher co-solvent concentration, the solubility and dissolution of ethanol into papaya leaves matrices largely influenced k_sa values to conform to larger internal mass transfer resistances instead. A similar observation was also observed by Solana et al. [18] where k_sa reduced with the increased in co-solvent flowrate. Table 4 summarized the findings of fitted parameters and mass transfer coefficients in BIC model.

Table 4. Model parameters calculated by BIC model approach.

Q (g/s)	y_r (g extract/g CO_2)	G	t_k (s)	k_fa (m^2/s)	k_sa (m^2/s)	AARD (%)
0.054	0.00051	0.144	5470	4.40x 10^{-5}	19.92 x 10^{-5}	6.87
0.081	0.00058	0.221	3094	5.869x 10^{-5}	11.55 x 10^{-5}	8.95
0.108	0.00058	0.258	1823	7.33 x 10^{-5}	6.76 x 10^{-5}	10.19
Overall AARD						8.67

4 Conclusions

The fittings of broken-intact-cell model for the extractions of papaya leaves by SCO_2 in the presence of co-solvent ethanol were represented. Three distinct observations were made in this study, firstly, the pressure variance within the system do not affect values of k_fa at constant flowrate, secondly the values of k_sa decreased at higher solvent flowrate, and thirdly the influence of k_fa values is proportionate to solvent flowrate introduced into the system. Furthermore, higher solvent flowrate improves the solubility of extract in SCO_2 with shorter time, t_k, required to extract easily accessible solutes. The role of co-solvent was also observed to play a significant role in the intraparticle mass transfer phenomenon.

The authors would like to gratefully express their sincere appreciation for the financial support from Fundamental Research Grant Scheme (FRGS) (015MA0-004) research grant awarded by Ministry of Higher Education, Malaysia and the support from Ministry of Education Malaysia though HICoE award to CBBR is duly acknowledged.

References

1. K. S. Duba and L. Fiori, J. Supercrit. Fluids **98**, 33 (2015)
2. K. Abbas, A. Mohamed, A. Abdulamir, and H. Abas, Am. J. Biochem. Biotechnol. **4**, 345 (2008)
3. B. V. Owoyele, O. M. Adebukola, A. A. Funmilayo, and A. O. Soladoye, Inflammopharmacology **16**, 168 (2008)
4. A. A. Mahmood, K. Sidik, and I. Salmah, Int. J. Mol. Med. Adv. Sci. **1**, 398 (2005)
5. N. Otsuki, N. H. Dang, E. Kumagai, A. Kondo, S. Iwata, and C. Morimoto, J. Ethnopharmacol. **127**, 760 (2010)
6. C. L. Cantrell, A. M. P. Jones, and A. Ali, J. Agric. Food Chem. **64**, 8352 (2016)
7. Y. H. Chai, S. Yusup, M. S. H. Ruslan, and B. L. F. Chin, Chem. Eng. Res. Des. **156**, 31 (2020)
8. H. Sovova, Chem. Eng. **49**, 409 (1994)
9. A. Mouahid, C. Crampon, S. A. A. Toudji, and E. Badens, J. Supercrit. Fluids **77**, 7 (2013)
10. O. Döker, U. Salgin, I. Şanal, Ü. Mehmetoğlu, and A. Çalimli, J. Supercrit. Fluids **28**, 11 (2004)
11. S. G. Özkal, M. E. Yener, and L. Bayındırlı, J. Supercrit. Fluids **35**, 119 (2005)
12. A. Rai, B. Mohanty, and R. Bhargava, Innov. Food Sci. Emerg. Technol. **38**, 32 (2016)
13. S. G. Ozkal, J. Am. Oil Chem. Soc. **86**, 1129 (2009)
14. A. C. Kumoro and M. Hasan, **15**, 877 (2007)
15. S. H. Soh and L. Y. Lee, 1 (2019)
16. S. G. Özkal and M. E. Yener, J. Supercrit. Fluids **112**, 76 (2016)
17. S. Machmudah, A. Sulaswatty, M. Sasaki, M. Goto, and T. Hirose, J. Supercrit. Fluids **39**, 30 (2006)
18. M. Solana, I. Boschiero, S. Dall'Acqua, and A. Bertucco, J. Supercrit. Fluids **94**, 245 (2014)